ARTICLES

An Examination of the Expectation Value Profiles for Average Stretch and Momentum in O−H and O−D Bonds of the HOD Molecule To Determine Their Role in Selective Photodissociation

Manabendra Sarma,[†,‡] S. Adhikari,[†,§] and Manoj K. Mishra*[,†]

Department of Chemistry, Indian Institute of Technology Bombay, Powai 400 076, India, Department of Chemistry, Indian Institute of Technology Guwahati, Guwahati 781 039, India, and Department of Physical Chemistry, Indian Association for the Cultivation of Science, Jadavpur, Kolkata 700 032, India

Received: April 28, 2008; Revised Manuscript Received: September 8, 2008

The expectation values for stretch and momentum in O−H and O−D bonds of the H−O−D molecule subjected to UV pulses effecting selective cleavage of these bonds have been analyzed to decipher the mechanistic basis of selective dissociation. Fully quantum dynamical calculations using both the ground and excited potential energy surfaces with different initial states and UV pulses reveal that prior stretch in a bond before transferring it to the repulsive first excited-state ensures preferential dissociation of this bond. The sampling of large stretch values and a quick downhill motion in the channel corresponding to dissociation of the prestretched bond on the upper surface are seen to underlie this preferential dissociation.

1. Introduction

Laser-assisted selective control of products from a chemical reaction is a subject of much importance and intense interest.[1−10] The local mode character of the O−H and O−D bonds in HOD and availability of accurate potential energy and dipole moment surfaces has made HOD a popular candidate for detailed investigation of selective bond dissociation.[11−36] The first excited $^1B_1$ electronic state of HOD is purely repulsive with a saddle point barrier separating the H + O−D and H−O + D channels. Excitation to the $^1B_1$ surface causes negligible change in the bending angle and use of preexcited O−H/O−D bonds in the ground electronic state with appropriate laser pulses which will deposit HOD in the desired dissociative channel on the repulsive upper surface has been an effective route to selective bond cleavage in HOD.[12−14,16−22,26−29,31,36] These features have made it possible to examine selective dissociation of O−H and O−D bonds using only the ground and first excited potential energy surfaces using reasonable UV pulses[12−16,22,24,27−30,32−35] in considerable detail and the preferential dissociation of O−H and O−D bonds in H + O−D ← H−O−D → H−O + D has served as a popular prototype for selective photodynamic control of chemical reactions.

Detailed investigation of the mechanism underlying preferential dissociation has however not received as much attention and the few attempts dedicated to this topic[13,14,16,22,28−31] have been mostly based on semiclassical Franck−Condon notions about depositing the HOD molecule in the required dissociating channel on the repulsive $^1B_1$ surface with prior stretch in the bond to be dissociated as an effective facilitator.[13,14,16,29−31] The different mechanistic visions resulting from these investigations have provided valuable insights into selective control in this important prototype, but due to classical/semiclassical approaches or idealized pulse types utilized in their enunciation,[13,14,16,22,28−31] a fully quantum mechanical investigation using both the ground and the excited surface and different initial states subjected to nonultrashort pulses is desirable.

We have mapped the H + O−D/H−O + D branching ratio as a function of UV field frequency for different initial states $|m, n\rangle$ (with m and n quanta of vibrational excitation in the O−H (m) and O−D (n) modes) and have established UV frequency regimes and initial states which will provide markedly selective dissociation of O−H/O−D bond as desired.[33−36] Fully quantal calculations with nonidealized UV pulses which do not assume instantaneous transfer from the ground to excited surface but take into account the field-induced cross-talk between the two surfaces have been shown to provide an effective route to selective[35,36] photodynamic control of bond dissociation in H−O−D. It is our purpose in this paper to map the time evolution of the expectation values of stretch and momenta on both the ground and the excited surface under conditions favoring different outcomes to try and analyze the role of stretch/momentum in effecting preferential control.

A brief outline of the computational considerations is presented in the following section. Discussion of the results and proposed mechanism is given thereafter, and a summary of main observations concludes this paper.

2. Method

The method employed here is identical with that employed in our earlier investigations,[33−36] and as in other previous investigations,[12−14,16,17,20,22,24,27−30,32] we too have considered only the ground and first excited electronic states with bending angle frozen at its equilibrium value. Rotational motion has been

* To whom correspondence should be addressed. E-mail: mmishra@iitb.ac.in. Fax: +91-22-2576-7152.
† Indian Institute of Technology Bombay.
‡ Indian Institute of Technology Guwahati.
§ Indian Association for the Cultivation of Science.

10.1021/jp803690r CCC: $40.75
Published on Web 11/21/2008

neglected as we are studying events on a femtosecond scale. The time evolution of the molecule with these assumptions is given by[22,29]

$$i\hbar\frac{\partial}{\partial t}\begin{pmatrix}\Psi_g\\ \Psi_e\end{pmatrix}=\begin{pmatrix}\hat{H}_g & \hat{H}_{uv}(t)\\ \hat{H}_{uv}(t) & \hat{H}_e\end{pmatrix}\begin{pmatrix}\Psi_g\\ \Psi_e\end{pmatrix} \quad (1)$$

where $\Psi_g = \Psi_g(r_1, r_2, t)$ and $\Psi_e = \Psi_e(r_1, r_2, t)$ are nuclear wave functions with subscripts referring to ground and first excited electronic states. r_1 and r_2 represent bond lengths along O−H and O−D coordinates. $\hat{H}_g = \hat{T} + \hat{V}_g$ and $\hat{H}_e = \hat{T} + \hat{V}_e$ are the Hamiltonians for ground and excited electronic states where $\hat{T}$ and $\hat{H}_{uv}$ are defined elsewhere.[22] The potential energy surfaces (PESs) $\hat{V}_g$ and $\hat{V}_e$ are obtained from refs 13 and 36 and refs 37 and 38, respectively. Equation 1 shown above is solved using Ψ_g as a vibrational state of the ground electronic state of HOD with initial condition $\Psi_e = 0$, at $t = 0$. The potential energy surfaces[14,37−39] and dipole moment surfaces[16,22,39,40] used in previous investigations[12−14,16,17,20,22,24,27−30,32−36] have been retained in the present study to enable meaningful comparison with earlier results.

The vibrational eigenfunctions which are to be used as Ψ_g for further study of HOD are obtained using the two-dimensional Fourier grid Hamiltonian (FGH) method.[41] Lanczos scheme[42] has been applied for time propagation of wave functions $\Psi_g(t)$ and $\Psi_e(t)$ whereas the effect of kinetic energy operators on the wave functions is evaluated using a two-dimensional fast Fourier transform (FFT).[43] The average bond lengths and momenta for O−H and O−D modes on ground and excited states are calculated as follows

average bond length

$$\langle r_i^j(t)\rangle = \frac{\langle\Psi_j(t)|r_i^j|\Psi_j(t)\rangle}{\langle\Psi_j(t)|\Psi_j(t)\rangle} \quad (2)$$

and average momentum

$$\langle p_i^j(t)\rangle = \frac{\langle\Psi_j(t)|p_i^j|\Psi_j(t)\rangle}{\langle\Psi_j(t)|\Psi_j(t)\rangle} \quad (3)$$

where the subscript i refers to either the O−H or the O−D bond. The superscript j refers to ground (g) or excited (e) electronic states.

We have used a two-dimensional spatial grid with individual coordinate r_{O-H} and r_{O-D} ranging from 1 a_0 to 10 a_0. In each dimension, grid is discretized using 128 grid points with equal grid spacing. As in our previous studies,[33,35,36] we have used a Gaussian UV pulse,[22]

$$E(t) = 0.09a(t)\cos\omega t$$

where the field envelope $a(t) = \exp[-\gamma(t - t_{uv})^2]$ with

$$\text{fwhm} = \sqrt{\frac{4\ln 2}{\gamma}} = 50 \text{ fs}$$

The temporal studies involved propagation for 10340 time steps (∼250 fs) with $\Delta t = 1$ au of time ≃0.0242 fs. The maximum field amplitude and corresponding field intensity of the laser pulse used here are 0.46 GV/cm and 178 TW/cm^2, respectively, being same as those used in earlier studies.[33,35,36] We have chosen a UV pulse with 50 fs fwhm to ensure a sufficiently narrow frequency bandwidth such that mechanistic analyses based on participation of individual vibrational levels remains feasible. We should mention that the chosen intensity for the UV pulses is fairly high and may give rise to non-negligible ionization. However, since we intend to provide a fully quantum mechanical test of premises put forward in earlier papers,[29,30] the intensities chosen by us are similar to that employed for this system by other researchers, e.g., Møller et al.[32] used a δ-function/5 fs pulse with an UV pulse of 56 TW/cm^2 maximum intensity and Elghobashi et al.[29] have used an UV pulse of 300 TW/cm^2 maximum intensity. The UV intensity used by us therefore is similar to or less than that employed by other researchers. Furthermore, at low UV field intensity there is hardly any stretch, and the proposition that we wish to test, i.e., the role of prior stretch in selective control of bond dissociation, becomes infructuous.

The time-integrated total flux in the competing channels, H + O−D and H−O + D, is calculated according to the following equations[33−36]

$$J_{H+O-D} = \int_0^{r_{2d}}\int_0^T \Psi^*(r_1, r_2, t)\left(\hat{j}_1 + \frac{\mu_2\cos\theta}{m_o}\hat{j}_2\right)\Psi(r_1, r_2, t)\,dr_2\,dt \quad (4)$$

and

$$J_{H-O+D} = \int_0^{r_{1d}}\int_0^T \Psi^*(r_1, r_2, t)\left(\hat{j}_2 + \frac{\mu_1\cos\theta}{m_o}\hat{j}_1\right)\Psi(r_1, r_2, t)\,dr_1\,dt \quad (5)$$

where $\hat{j}_i$ is the flux operator in the ith channel, defined as

$$\hat{j}_i = \frac{1}{2\mu_i}[\hat{p}_i\delta(r_1 - r_i^d) + \delta(r_i - r_i^d)p_i]$$

μ_i, $\hat{p}_i$, and r_i^d are the reduced mass, the momentum operator, and a grid point in the asymptotic region of the ith channel. At a time, we will consider one vibrational state of the molecule as our initial condition and the flux in H + O−D/H−O + D channels are evaluated along asymptotic cuts at $r_{O-H} = r_{O-D} = 7.5a_0$. An absorbing ramp potential is used at the asymptotic cuts to avoid unphysical reflection from the edges.

3. Results and Discussion

The carrier frequency for the Gaussian UV pulse profile discussed above is chosen to maximize selective photodissociation depending on the initial vibrational state of the HOD molecule on the ground electronic state and the results using an UV field of 67169 cm^{-1} frequency with $|0, 0\rangle$ as the initial state are presented in Figure 1. Figure 1b provides the pattern for population transfer from ground to excited surface and the resulting flux in the H + O−D and H−O + D channels on the upper surface. It can be seen from Figure 1b that, as the field begins to gain sufficient strength from 40 fs onward, there is a rapid population transfer from ground to excited electronic state and the population build up in the excited state goes on until approximately 60 fs at which time the flux in H + O−D channel begins to pick up. This is because the upper excited surface is entirely repulsive[37,38] and any population deposited in totally repulsive H + O−D or H−O + D channels of the excited surface is bound to lead to the dissociative downhill motion in both the channels and a build up of flux at the cost of diminution of population.

What is seen only faintly in Figure 1b but much more so in Figures 2b, 3b, 4b, and 5b is a field-induced cross-talk between the ground and the excited electronic state populations, and as the flux (J_{H+O-D}) builds up from 65 to 80 fs in Figure 1b, there is, as expected, a sharp decrease in the excited-state population which is being flushed out as dissociative flux in H + O−D and H−O + D channels. Beginning at 65 fs, the cross-talk

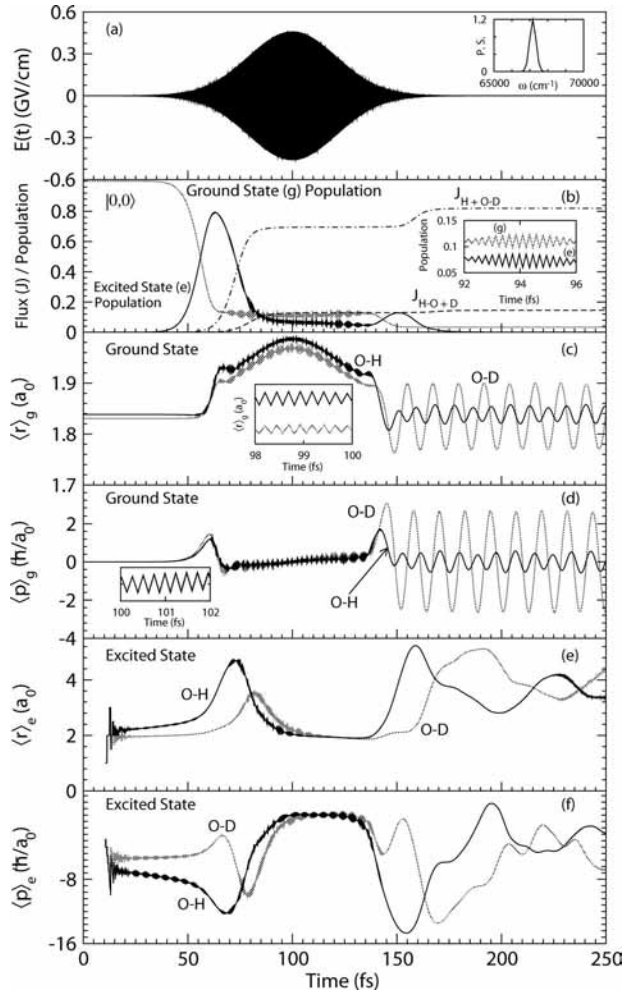

Figure 1. Results from exposure of the ground vibrational state $|0, 0\rangle$ of HOD on ground electronic state to the (a) Gaussian UV pulse $E(t) = 0.09 \exp[-\gamma(t - t_{uv})^2](\cos \omega t)$ with fwhm $= ((4 \ln 2)/\gamma)^{1/2} = 50$ fs, $t_{uv} = 100$ fs, and $\omega = 67169$ cm^{-1}. The power spectrum (P.S.) is provided as inset. (b) Ground- and excited-state populations and accumulated H + O−D and H−O + D flux. (c) Average bond lengths $\langle r \rangle_g$ on ground surface for O−H and O−D bond modes. (d) Average momenta $\langle p \rangle_g$ on ground surface for O−H and O−D modes (e) Average bond lengths $\langle r \rangle_e$ on excited surface. (f) Average momenta $\langle p \rangle_e$ on excited surface.

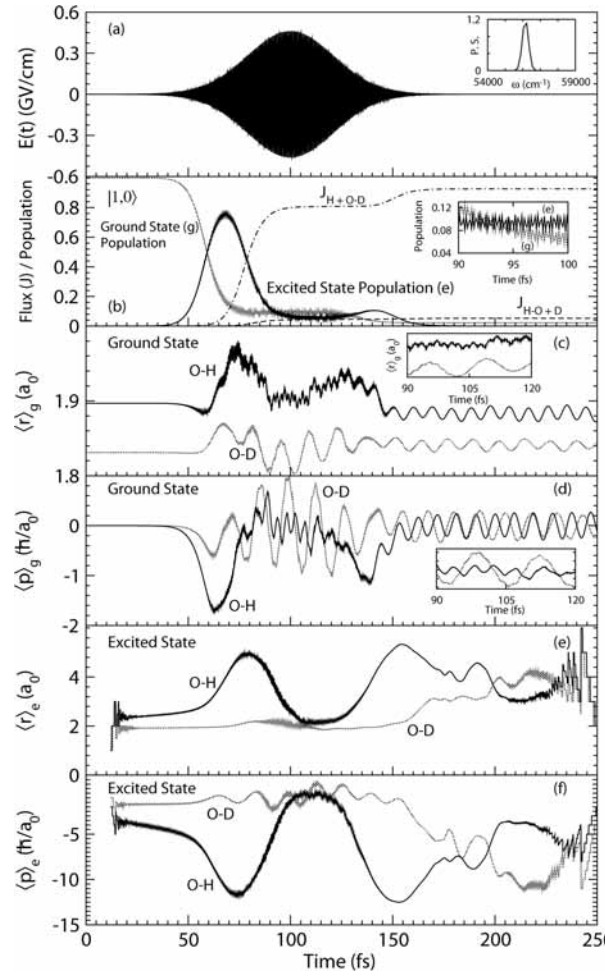

Figure 2. Results from exposure of the $|1, 0\rangle$ vibrational state of HOD on ground electronic state to the same Gaussian UV pulse as in Figure 1 but with $\omega = 56155$ cm^{-1}. (a−f) Same as in Figure 1.

between two surfaces is quite significant, by 90 fs, the flux in H+O−D has built up to 72%, and there is more or less stable population in ground and excited states as also stable flux in the two channels which does not change until the field is more or less switched off at 150 fs. As the field is switched off, the field-induced cross-talk stops and the population in the excited state comes down quickly to near zero with a kick up in the H + O−D flux and a near total dissociation of the H−O−D molecule with ∼82% flux (J_{H+O-D}) in the H + O−D channel and ∼15% (J_{H-O+D}) in H−O + D channel.

Between 80 and 140 fs, there is almost stable flux in both H + O−D and H−O + D channels, and as a result, population in the ground and excited states is also nearly stable but with persistent cross-talk. The stability of flux implies that, on the excited state, the bond stretching must be in the near vicinity of the equilibrium $\langle r_{O-H} \rangle$ and $\langle r_{O-D} \rangle$ values as seen in the excited-state stretch expectation value profile of Figure 1e. The near constant stability of features between 100 and 150 fs in the excited-state expectation values of panels e and f of Figure 1 is therefore linked to an absence of flux build up and the stable cross-talk between ground- and excited-state populations in this interval where the probability density profile on the excited-state surface remains anchored near equilibrium $\langle r_{O-H} \rangle$ and $\langle r_{O-D} \rangle$ values on the excited-state surface (as seen in 100−150 fs plots of Figure 2 in an earlier paper).[35] However, as also seen in 100−150 fs plots of the same figure[35] there is considerable sloshing around in the ground-state probability density profiles. This sloshing around in ground-state probability density profile induced by the cross-talk between the ground and the excited-state populations indicates that the dumping from the excited surface is not always to the ground vibrational state of the ground electronic state and the field-induced dumping from the upper excited electronic surface may also be to excited vibrational levels of the ground surface which leads to the mixing of higher vibrational excited states in the ground-state populations which we believe is responsible for the additional field induced stretching in the 80−140 fs interval of Figure 1c where other expectation values are stable. Of course, as the field is switched off around 150 fs, the kick up in the flux seen in Figure 1b is through a complicated downhill sloshing in repulsive H + O−D and H−O + D channels on the excited surface giving rise to the sampling of larger $\langle r_{O-H} \rangle$ and $\langle r_{O-D} \rangle$ values in Figure 1e. On the ground electronic surface, the stretch in the O−H and O−D bonds reverts to oscillations around the equilibrium values once the field has been switched off. The ground-state stretching expectation value profile after the field is switched off is oscillatory in Figure 1c, and there is a classical complementarity between the stretch/momentum expectation

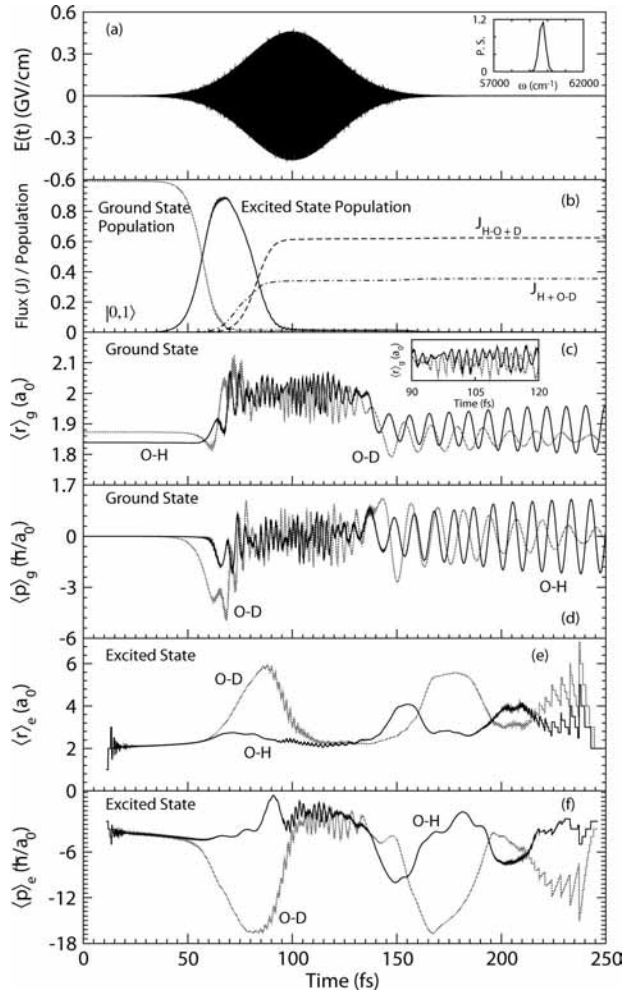

Figure 3. Same as Figure 2 except initial state is $|0, 1\rangle$ and $\omega = 59703$ cm^{-1}.

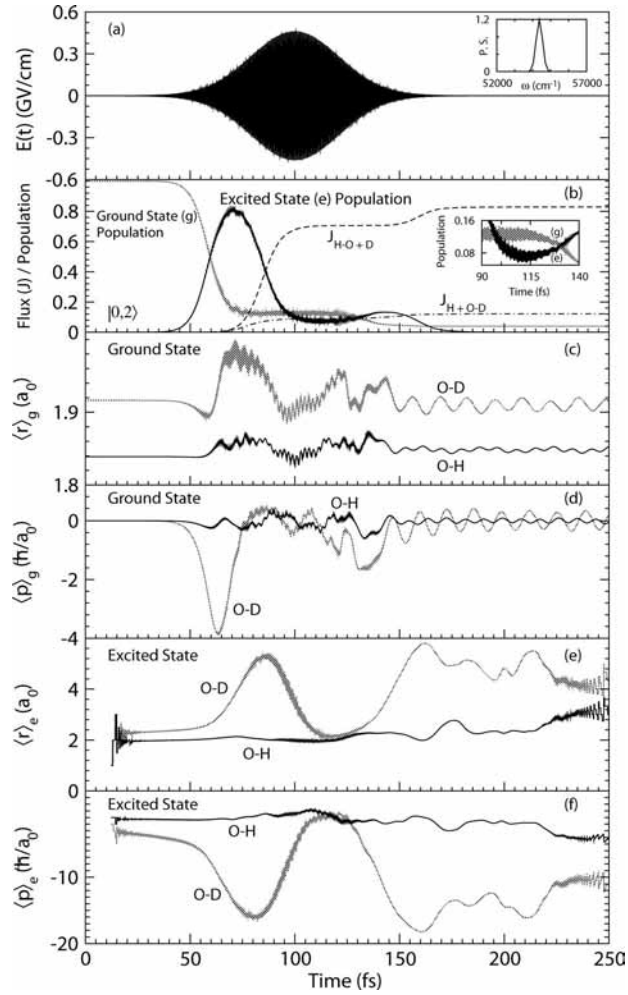

Figure 4. Same as Figure 2 except initial state is $|0, 2\rangle$ and $\omega = 54372$ cm^{-1}.

value profiles of panels c and d and e and f of Figure 1. The features discussed for Figure 1 become more pronounced and easily discernible in Figures 2−5.

As can be seen from panels a and c of Figure 1, the onset of buildup in field strength leads to a concerted buildup of stretch in both the O−H and the O−D bonds which normalize to expected low amplitude oscillations as the field is switched off with lower energy O−D bond showing larger amplitude motion. The inset makes it clear that for the ground vibrational state $|0, 0\rangle$, O−H and O−D stretch/contraction are synchronized with the field-induced stretch being slightly more in the O−H bond, and as long as the field is on, the finer undulations in the inset are also larger for the O−H bond as expected. The corresponding average momentum profiles in the ground vibrational state for the two bonds are plotted in Figure 1d, and the field-induced average momentum distributions in the two bonds on the ground surface are coupled and comparable. Though, the field-induced flux in Figure 1b is clearly higher for break up of O−H bond, this does not seem to ensue from any buildup of much larger momentum in this bond in comparison to the O−D bond. The long time field-free average momentum profile for both the bonds mirror the average stretch profile of Figure 1c.

The real reason for higher H + O−D flux is made clear by panels e and f of Figure 1 where a small bias toward greater initial stretch in the O−H bond on the ground surface (Figure 1c) leads to a quick downhill motion (larger negative momentum) of Figure 1f in the H + O−D valley on the upper surface, sampling dissociation limit average stretch in the excited state (Figure 1e) which is much larger and quicker for the O−H bond, and our results seem to clearly favor a critical role for an initial bias in bond stretch as an effective facilitator for selective dissociation of the O−H bond in this case. The variations in the average stretch and momentum profiles are a confirmation of the complexities in the downhill motion in the H + O−D and H−O + D valleys of the repulsive upper surface. Sloshing around of the wave function in these valleys is well established[13,14,16,17,20,22,27−29,31,33−36] and the excited-state average stretch and momentum profiles are a manifestation of this complex probability distribution in the dissociative downhill motion in the H + O−D and H−O + D valleys, on the upper repulsive surface.[33−36]

The dominant role of initial stretch in controlling the selective outcome of photodissociation is further examined by using the initial vibrational state $|1, 0\rangle$ with one quantum of vibrational excitation in O−H stretch. The flux in H + O−D rises from ∼82% with $|0, 0\rangle$ and 67169 cm^{-1} UV pulse to ∼93% with $|1, 0\rangle$ as the initial state and 56155 cm^{-1} UV pulse (Figure 2a) used to transfer the $|1, 0\rangle$ population in the ground state to the repulsive $^1B_1$ surface. The population transfer and flux profiles are presented in Figure 2b, and it is easily seen that the cross-talk between the ground and excited surface sets in as soon as the field strength builds up and is quite pronounced thereafter. This back and forth population exchange as the molecule samples different regions of the upper surface leads to a mixing

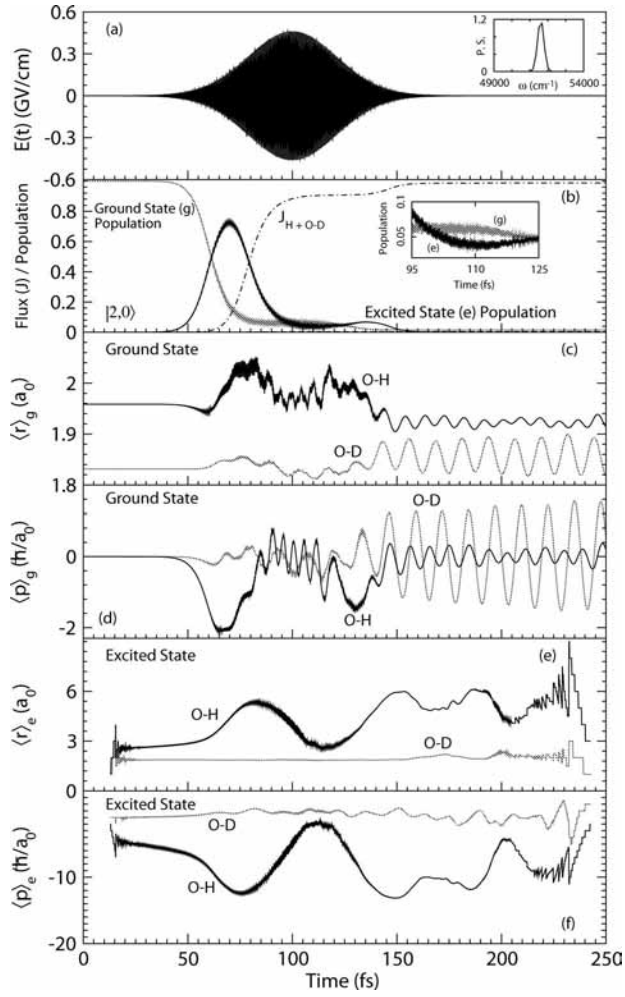

Figure 5. Same as Figure 2 except initial state is $|2, 0\rangle$ and $\omega = 51611$ cm^{-1}.

of vibrational states on the ground surface which is easy to see in the average stretch profile for the O−H bond on the ground surface plotted in Figure 2c which oscillate considerably. The large initial O−H stretch built into the $|1, 0\rangle$ state gives rise to a small initial contraction (Figure 2c) and a negative initial average momentum $\langle p_{O-H}\rangle$ in the beginning (Figure 2d). The $\langle r_{O-H}\rangle$ and $\langle p_{O-H}\rangle$ as also $\langle r_{O-D}\rangle$ and $\langle p_{O-D}\rangle$ profiles seem to show a near classical interlocking of the momentum maxima with stretch minima and the momentum minima with stretch maxima.

The large initial stretch in the O−H bond accentuates the effects seen earlier in panels e and f of Figure 1 where quick sampling of dissociatively large stretch regions of the excited state with bond lengths large enough to mimic dissociation (Figure 2e) and even larger average negative momentum (Figure 2f) than that seen for the $|0, 0\rangle$ state quickening the downhill motion in the H + O−D valley of the upper surface facilitates larger flux in the H + O−D channel. The extended features of the excited-state average stretch and momentum profiles (Figure 2, panels e and f) once again mirror the complex sloshing of the probability density flow on the upper surface.[33]

The results from Figures 1 and 2 favor a clinching role for initial stretch in selective photodynamic control of bond dissociation. This is as expected, since we have shown earlier[33] that starting from $|0, 1\rangle$ as the initial state with one quantum of vibrational excitation in the O−D bond reverses the kinematic bias in favor of preferential O−H dissociation. This proposition is examined in Figure 3 where larger flux in H−O + D channel of Figure 3b can be correlated with the larger initial stretch of the O−D bond seen in Figure 3c. However, since the difference between O−H and O−D stretches is not so large and there is substantive field-induced stretching (mixing of higher vibrations) (Figure 3c) in the O−H mode as well,[33] even though the UV frequency resonates with the $|0, 1\rangle$ state of HOD, there is considerable flux in the H + O−D channel (Figure 3b) and high-amplitude O−H oscillations prevail in longer time field-free regime (Figure 3c). The role of UV pulse resonating with the $|0, 1\rangle$ state is seen more in panels e and f of Figure 3 where the slight bias in average stretch for the O−D bond in the ground state (Figure 3c) translates into sampling of dissociatively large average O−D stretch values (Figure 3e) with fast downhill motion in the H−O + D valley (Figure 3f).

The premise favoring initial stretch-based selective control is further tested using two quanta of excitation in the O−D bond (Figure 4) which provides much larger initial stretch in comparison to the O−H bond as seen in Figure 4c and translates into flux values (∼83%) (Figure 4b) for H−O + D earlier seen with $|0, 0\rangle$ state for the H + O−D channel. The mechanistic details of panels c−f of Figure 4 are similar to those discussed earlier, and the results from use of the $|2, 0\rangle$ state with near 100% flux in the H + O−D channel presented in Figure 5 provide a comforting confirmation of the mechanistic route detailed earlier.

4. Concluding Remarks

We have attempted a detailed investigation of the change in average momentum and stretch in O−H and O−D bonds using different initial states and UV pulses most suited for their transfer from the ground to the repulsive upper surface. The larger stretch provided by prior vibrational excitation in the chosen bond is always seen to favor selective dissociation of that bond with near 100% selectivity if the chosen bond is stretched considerably more than the other bond. Since preparation of these initial states is much easier than trying to time the UV field such that it will be concurrent with maximum bond elongation, our results favor a prior stretched bond based selective photodynamic control of H + O−D ← H−O−D → H−O + D photodissociation.

The concerted use of detailed temporal profile of expectation values of bond stretch and momentum on both the ground and excited surfaces is seen to provide a clinching correlation between even small extra stretch in a bond facilitating the sampling of dissociative regions of the upper surface through accelerated downhill motion in the repulsive valley favoring its dissociation. The detailed quantum mechanical study presented here lends rigor to these insights into control mechanism for HOD and, we hope, will lead to their routine use in mechanistic investigation of selective control of other triatomic/polyatomic systems. An effort along these lines is underway in our group.

Acknowledgment. This research has been supported by grants from the Board of Research in Nuclear Sciences (Grant No. 2007/37/41-BRNS/2103) and Department of Science and Technology (DST) (Grant No. SR/S1/PC-30/2006), India to one of the authors (M.K.M.). M.S. is grateful to IIT Guwahati for a startup grant. M.S. acknowledges support from CSIR, India (SRF, F. NO. 9/87(336)/2003-EMR-I) and S.A. from Department of Science and Technology (DST), India, for partial financial support through project No. SP/S1/H-53/01.

References and Notes

(1) Lozovoy, V. V.; Zhu, X.; Gunaratne, T. C.; Harris, D. A.; Shane, J. C.; Dantus, M. *J. Phys. Chem. A* **2008**, *112*, 3789.
(2) Chakrabarti, R.; Rabitz, H. *Int. Rev. Phys. Chem.* **2007**, *26*, 671.
(3) Rabitz, H. *Science* **2006**, *314*, 264.
(4) Elles, C. G.; Crim, F. F. *Annu. Rev. Phys. Chem.* **2006**, *57*, 273.
(5) Shapiro, M.; Brumer, P. *Phys. Rep.* **2006**, *425*, 195.
(6) Shapiro, M.; Brumer, P. *Principles of the Quantum Control of Molecular Processes*; Wiley: New York, 2003.
(7) Henriksen, N. E. *Chem. Soc. Rev.* **2002**, *31*, 37.
(8) Rice, S. A. *Nature (London)* **2001**, *409*, 422.
(9) Rice, S. A.; Zhao, M. *Optical Control of Molecular Dynamics*; Wiley: New York, 2000.
(10) *Femtosecond Chemistry*; Manz, J., Wöste, L., Eds.; Verlag Chemie: Weinheim, 1995.
(11) Segev, E.; Shapiro, M. *J. Chem. Phys.* **1982**, *77*, 5604.
(12) Engel, V.; Schinke, R. *J. Chem. Phys.* **1988**, *88*, 6831.
(13) Zhang, J.; Imre, D. G. *Chem. Phys. Lett.* **1988**, *149*, 233.
(14) Zhang, J.; Imre, D. G.; Frederick, J. H. *J. Phys. Chem.* **1989**, *93*, 1840.
(15) Shafer, N.; Satyapal, S.; Bersohn, R. *J. Chem. Phys.* **1989**, *90*, 6807.
(16) Imre, D. G.; Zhang, *J. Chem. Phys.* **1989**, *139*, 89.
(17) Hartke, B.; Manz, J.; Mathis, *J. Chem. Phys.* **1989**, *139*, 123.
(18) Vander Wal, R. L.; Scott, J. L.; Crim, F. F. *J. Chem. Phys.* **1990**, *92*, 803.
(19) Bar, I.; Cohen, Y.; David, D.; Rosenwaks, S.; Valentini, J. J. *J. Chem. Phys.* **1990**, *93*, 2146.
(20) Vander Wal, R. L.; Scott, J. L.; Crim, F. F.; Weide, K.; Schinke, R. *J. Chem. Phys.* **1991**, *94*, 3548.
(21) Bar, I.; Cohen, Y.; David, D.; Arusi — Parper, T.; Rosenwaks, S.; Valentini, J. J. *J. Chem. Phys.* **1991**, *95*, 3341.
(22) Amstrup, B.; Henriksen, N. E. *J. Chem. Phys.* **1992**, *97*, 8285.
(23) Shapiro, M.; Brumer, P. *J. Chem. Phys.* **1993**, *98*, 201.
(24) Henriksen, N. E.; Amstrup, B. *Chem. Phys. Lett.* **1993**, *213*, 65.
(25) Cohen, Y.; Bar, I.; Rosenwaks, S. *J. Chem. Phys.* **1995**, *102*, 3612.
(26) Brouard, M.; Langford, S. R. *J. Chem. Phys.* **1997**, *106*, 6354.
(27) Campolieti, G.; Brumer, P. *J. Chem. Phys.* **1997**, *107*, 791.
(28) Meyer, S.; Engel, V. *J. Phys. Chem. A* **1997**, *101*, 7749.
(29) Elghobashi, N.; Krause, P.; Manz, J.; Oppel, M. *Phys. Chem. Chem. Phys.* **2003**, *5*, 4806.
(30) Henriksen, N. E.; Møller, K. B.; Engel, V. *J. Chem. Phys.* **2005**, *122*, 204320.
(31) Akagi, H.; Fukazawa, H.; Yokoyama, K.; Yokoyama, A. *J. Chem. Phys.* **2005**, *123*, 184305.
(32) Møller, K. B.; Westtoft, H. C.; Henriksen, N. E. *Chem. Phys. Lett.* **2006**, *419*, 65.
(33) Sarma, M.; Adhikari, S.; Mishra, M. K. *Chem. Phys. Lett.* **2006**, *420*, 321.
(34) Adhikari, S.; Deshpande, S.; Sarma, M.; Kurkal, V.; Mishra, M. K. *Radiat. Phys. Chem.* **2006**, *75*, 2106.
(35) Sarma, M.; Adhikari, S.; Mishra, M. K. *J. Chem. Phys.* **2007**, *127*, 024305.
(36) Sarma, M.; Mishra, M. K. *J. Phys. Chem. A* **2008**, *112*, 4895.
(37) Reimers, J. R.; Watts, R. O. *Mol. Phys.* **1984**, *52*, 357.
(38) Staemmler, V.; Palma, A. *Chem. Phys.* **1985**, *93*, 63.
(39) Engel, V.; Schinke, R.; Staemmler, V. *J. Chem. Phys.* **1988**, *88*, 129.
(40) Lawton, R. T.; Child, M. S. *Mol. Phys.* **1980**, *40*, 773.
(41) Dutta, P.; Adhikari, S.; Bhattacharyya, S. P. *Chem. Phys. Lett.* **1993**, *212*, 677.
(42) Leforestier, C.; Bisseling, R. H.; Cerjan, C.; Feit, M. D.; Friesner, R.; Guldberg, A.; Hammerich, A.; Jolicard, G.; Karrlein, W.; Meyer, H.-D.; Lipkin, N.; Roncero, O.; Kosloff, R. *J. Comput. Phys.* **1991**, *94*, 59.
(43) Kosloff, D.; Kosloff, R. *J. Comput. Phys.* **1983**, *52*, 35.

JP803690R